JOURNAL OF VIROLOGY, June 2007, p. 6276–6285 Vol. 81, No. 12
0022-538X/07/$08.00+0 doi:10.1128/JVI.02538-06


# Construction and Characterization of a Full-Length Infectious Simian T-Cell Lymphotropic Virus Type 3 Molecular Clone▽

Sébastien Alain Chevalier,[1]† Marine Walic,[1]† Sara Calattini,[1] Adeline Mallet,[2] Marie-Christine Prévost,[2] Antoine Gessain,[1] and Renaud Mahieux[1]*

*Unité d'Epidémiologie et Physiopathologie des Virus Oncogènes, CNRS URA 3015, Département de Virologie, Institut Pasteur, 28 rue du Dr. Roux, 75015 Paris, France,[1] and Plateforme de Microscopie Electronique, Institut Pasteur, 25 rue du Dr. Roux, 75015 Paris, France[2]*

Received 20 October 2006/Accepted 27 March 2007

**Together with their simian T-cell lymphotropic virus (STLV) equivalent, human T-cell lymphotropic virus type 1 (HTLV-1), HTLV-2, and HTLV-3 form the primate T-cell lymphotropic virus (PTLV) group. Over the years, understanding the biology and pathogenesis of HTLV-1 and HTLV-2 has been widely improved by the creation of molecular clones. In contrast, so far, PTLV-3 experimental studies have been restricted to the overexpression of the *tax* gene using reporter assays. We have therefore decided to construct an STLV-3 molecular clone. We generated a full-length STLV-3 proviral clone (8,891 bp) by PCR amplification of overlapping fragments. This STLV-3 molecular clone was then transfected into 293T cells. Reverse transcriptase PCR experiments followed by sequence analysis of the amplified products allowed us to establish that both *gag* and *tax*/*rex* mRNAs were transcribed. Western blotting further demonstrated the presence of the STLV-3 p24$^{gag}$ protein in the cell culture supernatant from transfected cells. Transient transfection of 293T cells and of 293T-long terminal repeat-green fluorescent protein cells with the STLV-3 clone promoted syncytium formation, a hallmark of PTLV Env expression, as well as the appearance of fluorescent cells, also demonstrating that the Tax3 protein was expressed. Virus particles were visible by electron microscopy. These particles are infectious, as demonstrated by our cell-free-infection experiments with purified virions. All together, our data demonstrate that the STLV-3 molecular clone is functional and infectious. This clone will give us a unique opportunity to study in vitro the different pX transcripts and the putative presence of antisense transcripts and to evaluate the PTLV-3 pathogenicity in vivo.**

Together with their simian T-cell lymphotropic virus (STLV) counterpart, human T-cell lymphotropic viruses (HTLVs) form the primate T-cell lymphotropic virus (PTLV) group (25). Until recently, only two HTLV types were known to occur in humans. We and others have lately reported the discovery of HTLV type 3 (HTLV-3) in two Cameroonese inhabitants (7, 63). The HTLV-3 sequence is highly related to Central African STLV-3 strains that are present in a number of monkey species living in that area (6, 55). The genomic organizations of HTLV-3 and STLV-3 proviruses are similar, with the presence of two long terminal repeat (LTR) sequences flanking the *gag*, *pol*, *env*, *tax*, and *rex* genes (6, 36, 37, 55, 58, 59). Of note, both the STLV-3 and HTLV-3 LTRs lack one Tax-responsive element compared to those of HTLV-1 or HTLV-2 (6, 36, 37, 55, 58, 59). Nevertheless, the PTLV-3 Tax protein can efficiently drive transcription from the PTLV-3 LTR as well as from the HTLV-1 and HTLV-2 LTRs (6, 11).

The number of open reading frames (ORFs) that are present in the PTLV-3 pX region is still a matter of debate; the STLV-3 prototype (STLV-$3_{PH969}$) pX region was reported to contain only one additional ORF, whose mRNA was amplified by reverse transcriptase PCR (RT-PCR) (57). In silico analyses suggested that this mRNA could be translated into a putative 84-amino-acid-long protein designated RORFII, which shares a number of similarities with the HTLV-1 p12$^{I}$ protein (57). However, the presence of RORFII mRNA was not detected when two other STLV-3 strain (PPA-F3 and CTO-604) pX transcripts were analyzed by RT-PCR (36, 37). Consequently, it is not clear whether, apart from Tax and Rex, additional ORFs are generally present in the STLV-3/HTLV-3 pX sequence.

Initial HTLV experimental studies have been restricted to an examination of infected patients (43), the overexpression of individual genes (mainly *tax*) using reporter assays (53, 54), or characterizations of HTLV-infected cell lines (44, 48). Although these studies were helpful, understanding the biology of HTLVs and their pathogenesis was later widely improved by the creation of HTLV-1 and HTLV-2 molecular clones (9, 12, 17, 19, 32, 39, 49, 50, 68) (for a review, see reference 3). Subsequently, deletion, point mutation, or domain-swapping analyses have allowed investigators to define more accurately the importance of a number of proteins encoded by the pX domain (for up-to-date reviews, see references 2 and 41), even though the recent discovery of an HTLV-1 antisense protein (HBZ) whose sequence partly covers the pX region (20) might imply that some of these results would benefit from being revisited.

The identification of factors that contribute to the potential pathogenicity of PTLV-3 would be feasible if a molecular clone that could be used in vitro and in vivo existed. The lack of

* Corresponding author. Mailing address: Unité d'Epidémiologie et Physiopathologie des Virus Oncogènes, CNRS URA 3015, Institut Pasteur, 28 rue du Docteur Roux, 75724 Paris cedex 15, France. Phone: (33)-1-45-68-89-06. Fax: (33)-1-40-61-34-65. E-mail: rmahieux@pasteur.fr.
† These authors contributed equally to this work.
▽ Published ahead of print on 11 April 2007.

TABLE 1. Sequence of the primers used for the amplification of the nine different STLV-3 PPA-F3 fragments

| Primer fragment | Sequences of primer set | Positions within the genome[a] | Annealing temp (°C) |
|---|---|---|---|
| E | GGGGGGGAATTCTGTCGATGATGATGAGCCCCG | 1→33 | 60.6 |
| | GGAGATCTTTCATTTGCCAGGGG | 1172←1150 | |
| G | TCTTAATTCAAGAAACCCCTGCGC | 999→1022 | 60.5 |
| | GGAGTGCTTGAATGCTAACAGGGG | 2122←2099 | |
| H | CCCAGCAGAAGCAGCCTATCC | 2048→2068 | 58.3 |
| | CGGAGAGCGAGATAGAGCTGG | 3247←3226 | |
| I | CTCTAAAGGCACCCCTGTCCTCCGC | 3191→3216 | 60.1 |
| | GAGACCGCCCCGGAGTAAGTATCCACCC | 4438←4411 | |
| F | CGTCACTCACCTCCAGTACAAGCG | 4364→4387 | 59.4 |
| | GGGCATTGTATAGCGCAGGGG | 5387←5367 | |
| D | GTATTCCCCCATTGGATAGCCAAACC | 5299→5324 | 60.9 |
| | GATGAGGAGGAGAAAGAGGGCC | 6429←6408 | |
| B | CTCTCCCAATGGGCCCGAGAAGCC | 6361→6384 | 59.9 |
| | TGTAGAGCTGAGCTGACAACG | 7433←7413 | |
| A | GGGGGGCTTTGTTCCGCTCGG | 7324→7344 | 62.6 |
| | CCTTCCTTGGGGCAAGGGCCG | 8021←8001 | |
| C | CTCCCGTGCCAAAAGGAAATTGCC | 7930→7953 | 60.3 |
| | TTTTTTTCGCGATGTTTGCTTTCTTCCCTAGGGCTAGC | 8891←8854 | |

[a] The direction of the arrow indicates the direction of transcription.

HTLV-3-infected cell lines and the restricted amount of HTLV-$3_{Pyl43}$ DNA that is available, combined with the strong sequence homologies between HTLV-$3_{Pyl43}$ and some STLV-3 strains, prompted us to construct an STLV-3 molecular clone. We describe here for the first time the construction of a full-length STLV-$3_{PPA-F3}$ provirus (8,891 bp), which was inserted into the SV2neo plasmid. SV2neo has previously been used for constructing an HTLV-2 molecular clone (51). Our results report for the first time a method for generating a full-length STLV-3 proviral clone. This clone (SV2neo$_{PPA-F3}$) produces infectious STLV-3 viral particles when transfected into 293T cells. SV2neo$_{PPA-F3}$ can now be used in vitro and in vivo. It will allow us to study the different pX transcripts in vitro. More importantly, it will give us a unique opportunity to investigate the tropism of the STLV-3 virus in vivo, the immune response following infection, and viral persistence.

## MATERIALS AND METHODS

**Cell culture.** 293T-LTR-green fluorescent protein (GFP) (15) and 293T cell lines were grown in Dulbecco's modified Eagle's medium (DMEM) supplemented with fetal bovine serum (10%) and antibiotics (penicillin, 100 U/ml; streptomycin, 100 μg/ml). Both cell lines were maintained at 37°C in 5% $CO_2$.

**Construction of the STLV-$3_{PPA-F3}$ molecular clone.** High-molecular-weight DNA was extracted (QIAmp DNA blood minikit; QIAGEN) from the blood of a *Papio anubis* monkey (PPA-F3) held at the Marseille CNRS cognitive primate center (Joel Fagot). Nine subgenomic overlapping fragments (A to I) representing the complete STLV-$3_{PPA-F3}$ proviral sequence (8,891 bp) were then amplified. The PCR mixtures contained 1 μg of DNA, 5 μl 10× *Pfu* buffer, a 0.2 mM concentration of each deoxynucleoside triphosphate (Roche), 2.5 U *PfuTurbo* DNA polymerase (Stratagene), and 10 pmol of each primer. Table 1 shows the primer sequences and the corresponding annealing temperatures. PCR products were purified on a 1% agarose gel (QIAquick gel extraction; QIAGEN) and cloned into the pCR2.1 vector (TA cloning; Invitrogen). Larger fragments (from E to F [fragment EF] and from F to C [fragment FC]) were then generated, as previously described (35). STLV-$3_{PPA-F3}$ provirus was inserted into the low-copy-number SV2neo plasmid. SV2neo encodes ampicillin resistance in bacteria and G418 resistance in mammalian cells (9, 49). Both SV2neo and SV2neo$_{PPA-F3}$ were grown in bacteria (SCS110; Stratagene) in the presence of ampicillin at 30°C in limited volumes in order to decrease the rate of recombination that frequently occurs in the presence of the LTR sequences.

At each step of the provirus construction, 6 to 10 clones were sequenced using the BigDye terminator kit and an ABI 3100 automated sequencer (Applied Biosystems) as described previously (6).

**RT-PCR.** Twenty-four hours posttransfection of 293T cells, total RNA was extracted with an RNeasy mini kit (QIAGEN) and treated twice with the DNase I RNase-free DNA set (QIAGEN) to avoid any carryover of the proviral plasmid (6). Total RNA (0.5 μg) was used as a matrix for RT-PCR with a one-step RT-PCR kit (QIAGEN). PCR was performed using the 602LTR and 602MVB Rex ex2 primers, which allow the amplification of a 424-bp PCR product corresponding to the spliced *tax*/*rex* mRNA (37). In a second series of RT-PCR experiments, *gag*-specific primers (Gsens, 5′TCTTAATTCAAGAAACCCCTG CGC3′, and Sc gag 1432 antisense, 5′TCTCCGAAGCCCTTGCTGATTTGG3′) were also used to amplify a 498-bp sequence.

**p19 ELISA.** Cell culture supernatant was collected at 24 and 48 h posttransfection and tested with the Retrotek HTLV-1/2 p19 antigen enzyme-linked immunosorbent assay (ELISA) (Zeptometrix). This kit allows the detection of the $p19^{gag}$ proteins of both HTLV-1 and HTLV-2 (1, 4).

**Western blotting.** 293T-LTR-GFP cells were transfected with the Polyfect reagent (QIAGEN) with 4 μg of SV2neo$_{PPA-F3}$, with 3 μg of SV2neo$_{PPA-F3}$ and 1 μg of pSG5M-$Tax3_{604}$, or with 4 μg of the SV2neo backbone vector. Ten days later, 10 ml of growth medium was collected, clarified by low-speed centrifugation (2,500 rpm for 5 min), and filtered through a 45-μm filter. Virus was then layered on a 20% glycerol gradient (18) and pelleted by centrifugation in a SW28 rotor at 22,000 rpm for 2 h. The pellet was resuspended in lysis buffer (50 mM Tris-HCl [pH 7.4], 120 mM NaCl, 5 mM EDTA, 0.5% NP-40, 0.2 mM $Na_3VO_4$, 1 mM dithiothreitol, 1 mM phenylmethylsulfonyl fluoride) in the presence of protease inhibitors (Complete; Boehringer). Cell debris were pelleted by centrifugation. The protein concentration was determined by the Bradford assay (Bio-Rad). Twenty microliters of each sample was resolved by electrophoresis on a 4 to 12% polyacrylamide-sodium dodecyl sulfate gel (NUPAGE; Invitrogen). Proteins were transferred to an Immobilon-P membrane (Millipore). Membranes were blocked in a 0.05% solution of phosphate-buffered saline (PBS)-

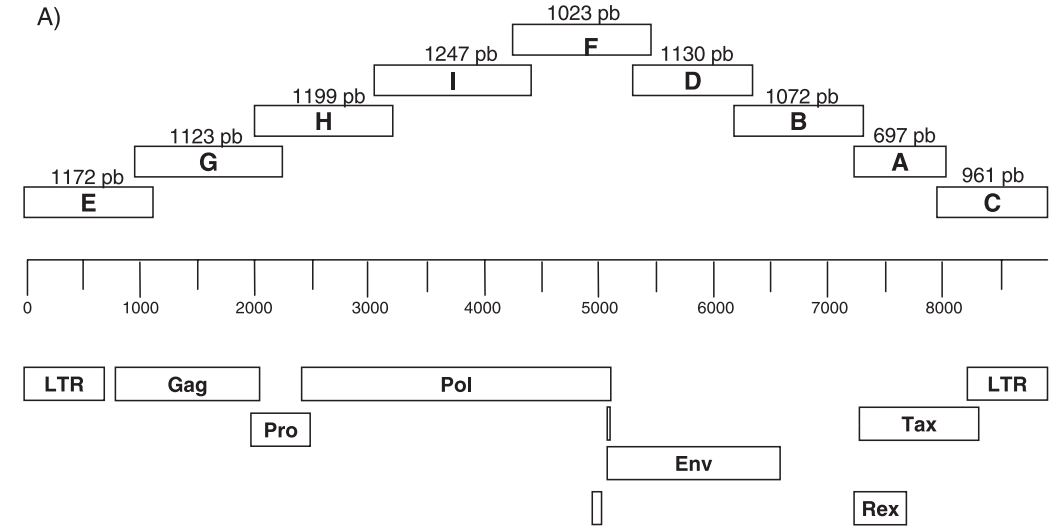
A)
1023 pb
F
1247 pb
I
1130 pb
D
1199 pb
H
1072 pb
B
1123 pb
G
697 pb
A
1172 pb
E
961 pb
C
0
1000
2000
3000
4000
5000
6000
7000
8000
LTR
Gag
Pol
LTR
Pro
Tax
Env
Rex

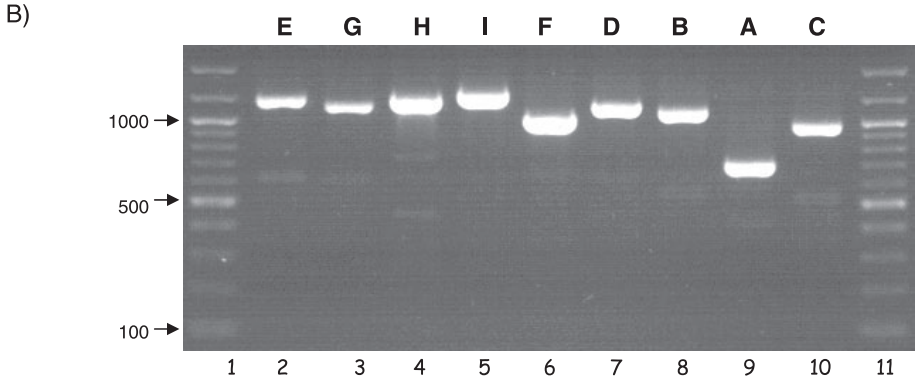
B)
E G H I F D B A C
1000
500
100
1 2 3 4 5 6 7 8 9 10 11

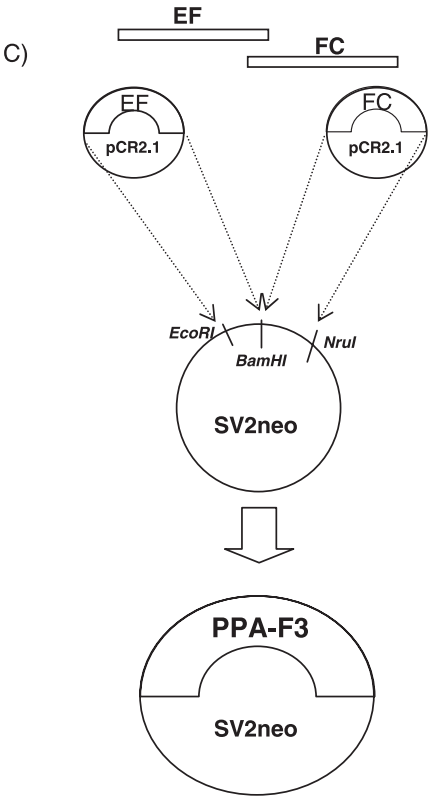
C)
EF
FC
EF
pCR2.1
FC
pCR2.1
EcoRI
BamHI
NruI
SV2neo
PPA-F3
SV2neo

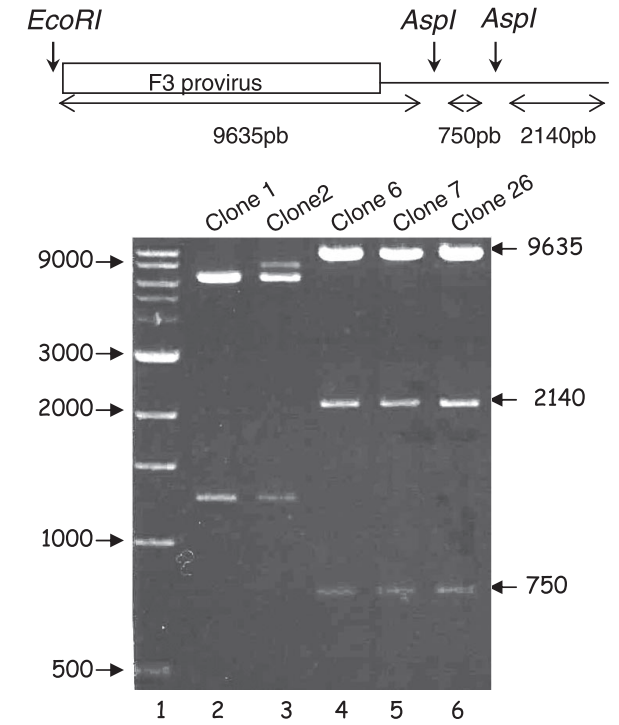
D)
EcoRI
AspI
AspI
F3 provirus
9635pb
750pb
2140pb
Clone 1
Clone2
Clone 6
Clone 7
Clone 26
9000
3000
2000
1000
500
9635
2140
750
1 2 3 4 5 6

Tween 20 with 5% milk and incubated with sera obtained from two STLV-3-infected primates (PPA-F8 or CTO-604 [data not shown]). The next day, the membranes were washed and incubated with anti-human horseradish peroxidase-conjugated secondary antibodies (P.A.R.I.S.) and developed using the SuperSignal West Femto chemiluminescent-substrate kit (Pierce).

**Immunofluorescence.** 293T-LTR-GFP cells were transfected with 2 μg of $SV2neo_{PPA-F3}$ using the Polyfect reagent (QIAGEN) as described previously (35). Three days later, cells were washed with PBS, fixed with 4% paraformaldehyde (Sigma), and visualized with a Zeiss Axioplan 2 imaging microscope (magnification, ×40) using a Zeiss Axiocam HRc (color) camera and the Zeiss ApoTome software as described previously (10).

**Secondary infection.** 293T cells were transfected twice (day 0 and day 1) with 4 μg of either $SV2neo_{PPA-F3}$ or the SV2neo empty vector, using the Polyfect reagent (QIAGEN). Forty-eight hours later, 8 ml of growth medium was collected from two 60-mm-diameter dishes and clarified by low-speed centrifugation (2,500 rpm for 5 min) then filtered through a 45-μm filter. Virus was then layered on a 20% glycerol gradient (18) and pelleted by centrifugation in a SW28 rotor at 22,000 rpm for 2 h. The pellet was then resuspended in 200 μl of DMEM without fetal bovine serum in the presence of 10 μg/ml of DEAE-dextran as previously described (17). As a control, the virus pellet was heated at 70°C for 2 h. 293T-LTR GFP indicator cells were incubated with 200 μl of the resuspended virus in a total volume of 2 ml of DMEM in the absence of fetal bovine serum for 2 h. Complete medium (8 ml) was then added and changed twice a week. One week later, live cells were visualized with a Zeiss Axioplan 2 imaging microscope (magnification, ×40) using a Zeiss Axiocam HRc (color) camera and the Zeiss ApoTome software as described previously (10).

**Syncytium formation.** 293T-LTR-GFP cells (15) were transfected with the Polyfect reagent (QIAGEN) with $SV2neo_{PPA-F3}$ or with the SV2neo empty vector. Forty-eight hours posttransfection, cell culture medium was removed, the cells were washed with PBS and fixed, and pictures were taken as described above.

**Electron microscopy.** For ultrastructural analyses, cells were fixed overnight at 4°C with 2.5% glutaraldehyde in 0.1 M cacodylate buffer, pH 7.4. Samples were postfixed with 1% osmium tetroxide in 0.1 M cacodylate buffer, pH 7.4, for 1 h and then with 2% uranyl acetate in 30% methanol for 1 h. Samples were then dehydrated in ethanol and embedded in epoxy resin. Ultrathin sections were stained with 2% uranyl acetate and lead citrate. Sections were examined using a Jeol JEM1010 transmission electron microscope (Jeol, Tokyo, Japan) at 80 kV and an Eloise MegaView III camera (Eloise SARL, Roissy, France).

## RESULTS

Because an STLV-3-infected immortalized or transformed cell line is not available to us, it was not possible to transfer the STLV-3 provirus from bacteriophage lambda to a plasmid vector, as previously reported for the construction of the HTLV-1 or of HTLV-2 molecular clones (9, 12, 17, 32, 39, 50, 51). For this reason, we chose a different approach that has been used for constructing full-length infectious foamy virus from subgenomic DNA fragments (62, 67). This method relies on the sequential addition of defined DNA fragments by PCR (Fig. 1A). To this end, we first amplified nine different partially overlapping sequences (A to I) from $STLV\text{-}3_{PPA-F3}$ high-molecular-weight DNA and cloned them into the pCR2.1 plasmid. The size of each fragment ranged from 961 bp to 1,247 bp (Fig. 1B). These nine pieces were then assembled into two larger fragments (EF and FC) by using a previously described technique (35), and ultimately, the complete genome was inserted into the SV2neo plasmid (Fig. 1C). SV2neo is a low-copy-number plasmid whose use drastically reduces the generation of deleted clones (3). Recombinant plasmids were screened by digesting the plasmid DNA with EcoRI and AspI (Fig. 1D, top panel). Among the plasmids tested, three clones display the expected restriction pattern, i.e., three bands at 9,636 bp, 2,140 bp, and 750 bp. Each of these recombinant plasmids therefore contains the full-length STLV-3 provirus (Fig. 1D, lower panel, lane 4 [clone 6], lane 5 [clone 7], and lane 6 [clone 26]). Each plasmid was then fully sequenced on both strands. Clone 26 (designated $SV2neo_{PPA-F3}$ throughout this article) was subsequently used for all analyses. In some cases, clones 6 and 7, which are also wild type in sequence, were used.

**Transfection of $SV2neo_{PPA-F3}$ and expression of viral mRNAs.** To determine whether the $SV2neo_{PPA-F3}$ molecular clone was capable of directing mRNA synthesis, total RNA was extracted from transiently transfected 293T cells, treated twice with DNase I, and subjected to RT-PCR to search for the presence of nonspliced *gag* or doubly spliced *tax*/*rex* viral messengers. As expected, a band corresponding to *gag* (498 bp) was present in 293T cells transfected with each of the $SV2neo_{PPA-F3}$ clones (i.e., clone 6, 7, or 26) but not in SV2neo or in mock-transfected cells (Fig. 2A, lanes 4, 5, and 6 versus lanes 2 and 3). The absence of amplicon when RT was omitted demonstrates the lack of DNA carryover in the RNA preparation (Fig. 2A, lane 7). All together, these results allow us to conclude that *gag* mRNA is present specifically in the $SV2neo_{PPA-F3}$-transfected cells.

We next determined whether *tax*/*rex* mRNA could also be detected (see Fig. 2B for the primer positions). A signal (424 bp) corresponding to part of the doubly spliced *tax*/*rex* messenger was specifically detected in $SV2neo_{PPA-F3}$-transfected 293T cells (Fig. 2C, lanes 46) to but not in SV2neo or in mock-transfected cells (Fig. 2B, lanes 2 and 3). We cloned and sequenced the 424-bp PCR product. Sequence analysis allowed us to demonstrate unambiguously that the PCR amplicon corresponded to the *tax*/*rex* mRNA (Fig. 2D). All together, these results demonstrate that both nonspliced and spliced mRNAs are transcribed following the transfection of $SV2neo_{PPA-F3}$ plasmid into 293T cells.

**Viral protein expression.** To determine whether viral proteins are translated, the supernatant of $SV2neo_{PPA-F3}$-transfected 293T cells was concentrated by ultracentrifugation and proteins were analyzed by electrophoresis using a monkey serum ($STLV\text{-}3_{PPA-F8}$) that has previously been shown to contain STLV-3 antibodies (36). A band corresponding to the STLV-3 $p24^{gag}$ protein was specifically observed in the supernatant

FIG. 1. Construction of the $SV2neo_{PPA-F3}$ molecular clone. (A) Representation of the nine partially overlapping $STLV\text{-}3_{PPA-F3}$ fragments used for the construction of the molecular clone and schematic representation of the $STLV\text{-}3_{PPA-F3}$ genome. The primers used for the PCR experiments are described in Table 1. (B) Analysis of the $STLV\text{-}3_{PPA-F3}$ amplified products cloned into the pCR2.1 vector. The PCR products (lanes 2 to 10) were analyzed on a 1% agarose gel. Lanes 1 and 11, 100-bp DNA ladder. Numbers at the left are in base pairs. The PCR product sizes are indicated in panel A. (C) The $STLV\text{-}3_{PPA-F3}$ genomic intermediates EF (5,387 bp) and FC (4,527 bp) were assembled into the SV2neo vector in order to obtain the complete $SV2neo_{PPA-F3}$ proviral genome. (D) Restriction map of the full-length $STLV\text{-}3_{PPA-F3}$ genome inserted into the SV2neo plasmid. Numbers at the left of the blot are in base pairs. Lane 1, 1-kb DNA ladder; lanes 2 to 6, recombinant plasmids digested with EcoRI and AspI that were on a 0.7% agarose gel. The expected restriction pattern consists of three bands at 9,636 bp, 2,140 bp, and 750 bp.

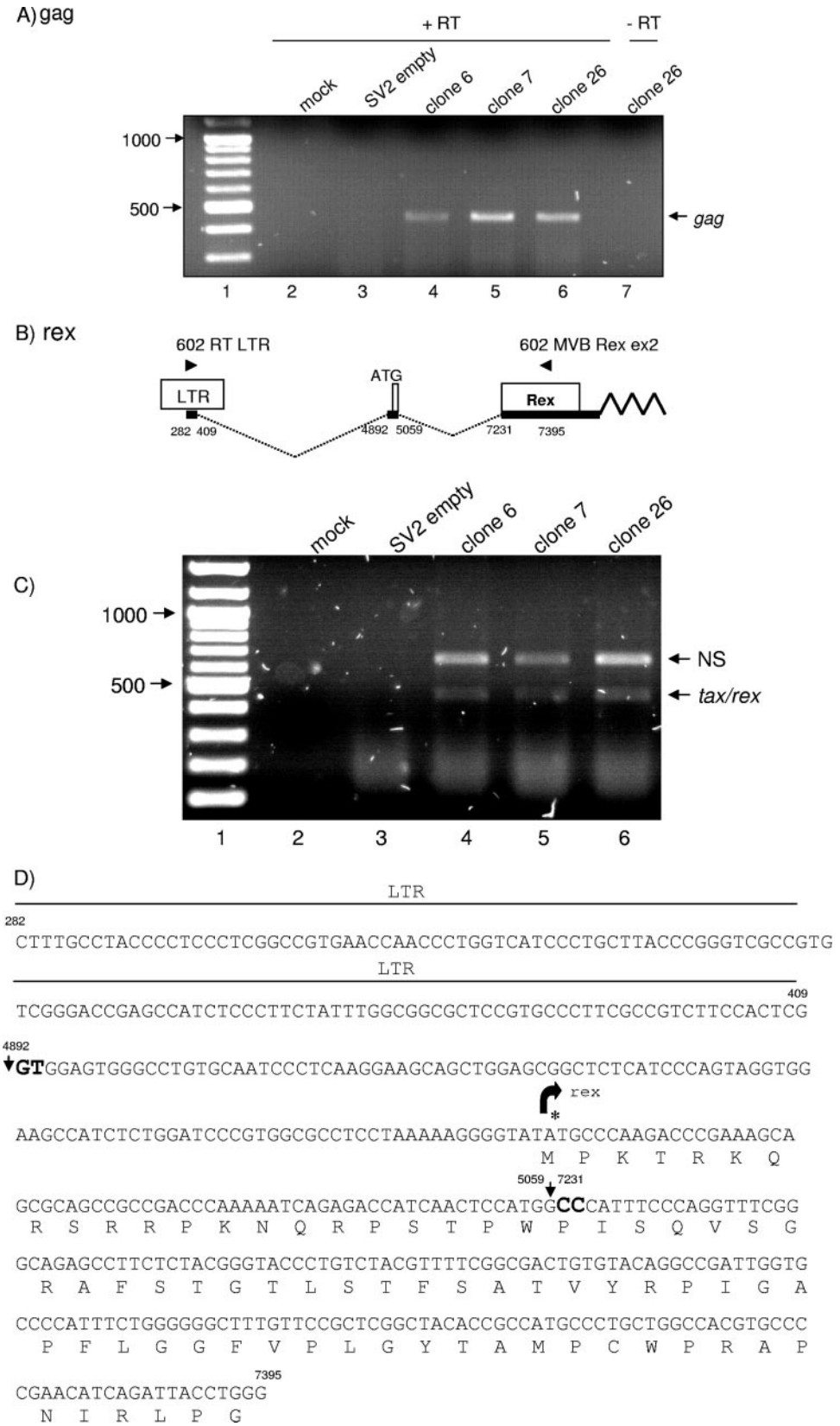


FIG. 2. RT-PCR analysis of viral SV2neo$_{PPA-F3}$ RNAs. Total RNA was extracted from transiently transfected 293T cells, treated with DNase I, and subjected to RT-PCR to search for the presence of (A) nonspliced *gag* (498-bp) or (B, C) doubly spliced *tax*/*rex* (424-bp) viral messengers. (A) Lane 1, 100-bp DNA ladder; lane 2, mock-transfected cells; lane 3, RNA from SV2neo-transfected cells; lanes 4 to 6, RNA from cells transfected with SV2neo$_{PPA-F3}$ clones 6, 7, and 26, respectively (these three recombinant plasmids contain the wild-type SV2neo$_{PPA-F3}$ sequence).

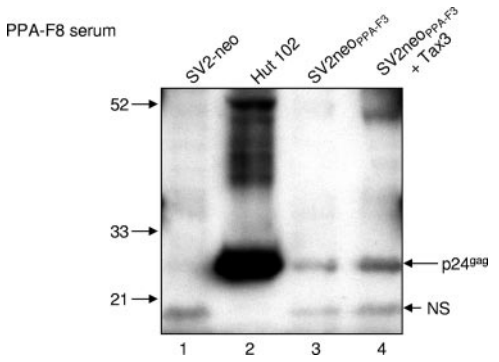


FIG. 3. Expression of virion structural p24$^{gag}$ protein released into the cell culture supernatant from 293T cells transfected with the SV2neo$_{PPA-F3}$ clone. 293T cells were transfected with SV2neo (lane 1), SV2neo$_{PPA-F3}$ (lane 3), or SV2neo$_{PPA-F3}$ plus pSG5M-Tax3 (lane 4). Ten days later, growth media were collected, clarified by low-speed centrifugation, and filtered. Virus was then layered on a 20% glycerol gradient and centrifuged. The pellet was then resuspended in lysis buffer. Each sample was resolved by electrophoresis on a 4 to 12% sodium dodecyl sulfate–polyacrylamide gel. Proteins were transferred to a membrane and incubated with a serum obtained from an STLV-3-infected primate (PPA-F8). For lane 2, HTLV-1 HUT-102 growth medium was also collected and processed under the experimental conditions described above. NS, nonspecific. This Western blot is representative of blots from two different experiments. Numbers at the left are in kilodaltons.

obtained from SV2neo$_{PPA-F3}$-transfected cells (Fig. 3, lane 3) but not in the protein extracts from SV2neo-transfected cells (Fig. 3, lane 1). To determine whether the simian Tax3 protein increased the production of viral antigens, the cells were also cotransfected with a Tax3 plasmid, as has been done previously for HTLV-1 molecular-clone experiments (32, 42). The presence of Tax3 modestly increased the amount of STLV-3 p24 in the cell supernatant (Fig. 3, lane 3 versus lane 4). All together, our results are similar to those of Green, who demonstrated previously that HTLV-2 sera detect mainly HTLV-2 p24$^{gag}$ in extracts from cells transfected with the pH6neo HTLV-2 molecular clone (23, 24). Overall, our results demonstrate that STLV-3$_{PPA-F3}$-transfected cells express STLV-3 p24$^{gag}$ protein. Similar Western blot results were obtained when the experiment was repeated with the serum from another STLV-3-infected animal (STLV-3$_{604}$ [data not shown]).

Interestingly, the STLV-3$_{PPA-F8}$ serum also cross-reacted with HTLV-1 p24$^{gag}$ protein present in HUT-102-infected cells (Fig. 3, lane 2). These results are consistent with previous reports which demonstrated that STLV-3 sera cross-react with HTLV-1 p24$^{gag}$ in a commercial Western blot assay (36, 37, 56, 59). We then performed the opposite experiment and tested whether commercial monoclonal or polyclonal anti-HTLV-1 p19$^{gag}$ or anti HTLV-1 p24$^{gag}$ cross-react with STLV-3 p19$^{gag}$ and p24$^{gag}$ proteins by Western blotting. While all of antibodies tested detected HTLV-1 p19$^{gag}$ and p24$^{gag}$ proteins present in HUT-102 HTLV-1-infected cells, none of them allowed the detection of STLV-3 p19$^{gag}$ or p24$^{gag}$ (data not shown). Therefore, so far, the STLV-3 sera are the only available source of anti-STLV-3 antibodies.

**p19$^{gag}$ detection.** We also tested whether SV2neo$_{PPA-F3}$ p19$^{gag}$ could be detected in the supernatant of STLV-3$_{PPA-F3}$-transfected cells using a commercial ELISA assay that has been widely used to detect p19$^{gag}$ in the supernatants of cells transfected with HTLV-1 or HTLV-2 molecular clones (16, 32, 40, 42, 52, 64). Although p19$^{gag}$ protein was easily measured in the supernatants of HUT-102, C8166, and C19 cells (HTLV-1 and HTLV-2, respectively), we measured only very small amounts of p19$^{gag}$ protein in supernatant samples from SV2neo$_{PPA-F3}$-transfected cells (data not shown). This value is not significantly higher than the background value. This result was in fact not entirely unanticipated, since (i) the Zeptometrix test has been built for detecting HTLV-1 and HTLV-2 p19$^{gag}$ and (ii) most STLV-3 sera do not cross-react with plates coated with the HTLV-1 p19$^{gag}$ protein from commercial Western blot assay kits (36, 37).

**Envelope expression and syncytium formation.** HTLV is transmitted mainly by cell-to-cell contact, which leads to the production of syncytia in vitro. Syncytium formation has been attributed to the interaction of the viral envelope on the surfaces of infected cells with the viral receptors that are present on the surfaces of adjacent cells (33). The ability of HTLV-1-infected cells (14, 27), of HTLV-2-infected cells (61), or of STLV-1-expressing cells (60) to form syncytia with target cells has been used as a model for cell-to-cell viral transfer. This phenomenon occurs in a broad range of cell lines (31). Since it is similar to other PTLVs, STLV-3 is expected to induce the formation of syncytia when amplified in tissue culture, if the infected cells express the envelope proteins (TM and SU) and the target cells express the STLV-3 receptor. To test this hypothesis, 293T cells were transfected with plasmid SV2neo$_{PPA-F3}$ or SV2neo. After 2 days of culture, syncytia were observed in the SV2neo$_{PPA-F3}$ cells (Fig. 4A, panel a), while this was not the case for cells that were transfected with the SV2neo backbone vector (Fig. 4A, panel b). These results demonstrate that upon transfection of the SV2neo$_{PPA-F3}$ plasmid in 293T cells, STLV-3 envelope proteins were translated. Ultimately, the STLV-3 SU protein bound to the STLV-3 receptor on the surfaces of 293T cells, and STLV-3 TM triggered the fusion between the donor and target cell membranes. Whether the STLV-3 receptor is glucose transporter-1, neuropilin-1 (21, 29, 34), or another cellular protein (30) is currently unknown.

**Tax expression.** We have previously demonstrated that the simian Tax3 protein transactivates the HTLV-1 LTR (11). To determine whether the SV2neo$_{PPA-F3}$ plasmid directs the ex-

For lane 7, RT was not added to the PCR mix containing RNA extracted from clone 26-transfected cells. (B) RT-PCR strategy for amplifying the *rex* transcript. The primers used and their positions were previously described (37). (C) RNAs were tested for the presence of a band corresponding to the spliced *tax*/*rex* mRNA transcript. Lane 1, 100-bp DNA ladder; lane 2, mock-transfected cells; lane 3, RNA from SV2neo-transfected cells; lanes 4 to 6, RNA from cells transfected with STLV-3$_{PPA-F3}$ clones 6, 7, and 26, respectively. NS, nonspecific band. (D) Sequence analysis of the 424-bp-long RT-PCR product. The *gag* and *tax*/*rex* gels are representative of at least three different experiments performed on different RNA preparations. Numbers to the left of the blots are in base pairs.

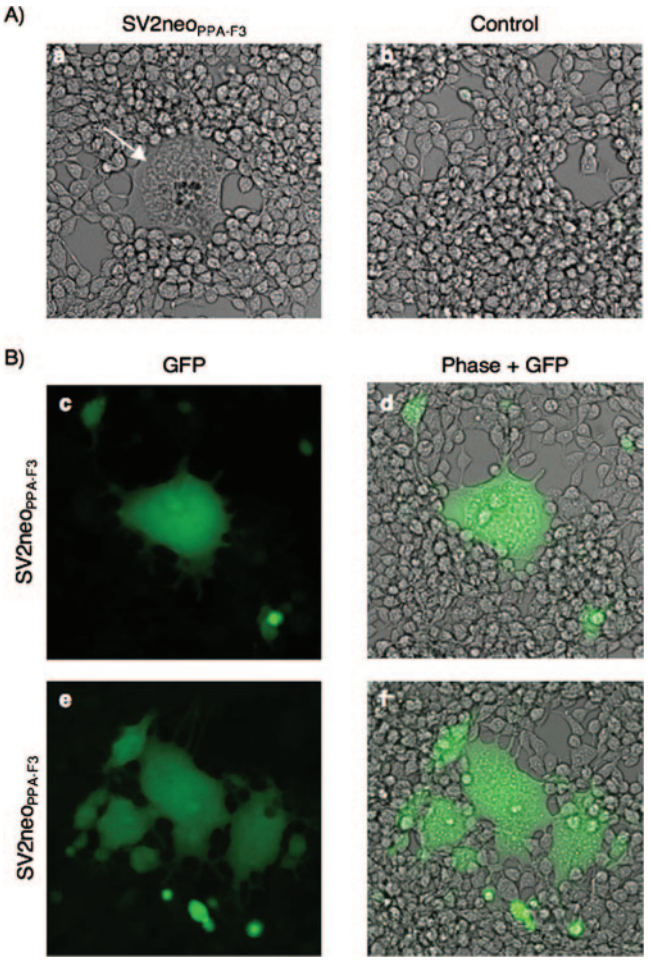


FIG. 4. Syncytium formation and Tax expression. (A) 293T cells were transiently transfected with (a) SV2neo$_{PPA-F3}$ or (b) the SV2neo empty vector. Forty-eight hours posttransfection, cell culture medium was removed, cells were washed with PBS and fixed, and pictures were taken with a Zeiss Axioplan-Axiocam-ApoTome system. (B, panels c to f) 293T-LTR-GFP cells were transiently transfected with SV2neo$_{PPA-F3}$. Forty-eight hours posttransfection, cells were processed as described above. (A and B) The images shown are representative of at least three different experiments.

pression of a functional Tax3 protein, indicator 293T–HTLV-1–LTR–GFP cells were transfected. Forty-eight hours later, a high number of fluorescent cells was observed (Fig. 4B, panels c to f), demonstrating that the Tax3 protein was expressed and functional. In most cases, the GFP signal was detected in cells that formed syncytia, confirming the expression of both the Env and Tax proteins within the same cells (Fig. 4B, panels d and f). As expected, neither the GFP signal nor syncytia were detected in the cells that had been transfected with the SV2neo backbone vector (data not shown).

**SV2neo$_{PPA-F3}$ produces viral particles.** SV2neo$_{PPA-F3}$-transfected 293T cells were observed by transmission electron microscopy to search for STLV-3$_{PPA-F3}$ viral particles. Microscope analysis revealed the presence of viral particles (Fig. 5a to c) whose sizes were not homogeneous (80 to 110 nm) and whose cores were of various densities, as previously reported for HTLV-1-infected cells (data not shown and reference 38), for cells transfected with an HTLV-2 molecular clone (data not shown), and for a short-term culture of STLV-3-infected cells (22). An envelope is visible in an enlarged image of Fig. 5a. These particles are very similar to those observed in MT2 cells or in 293T cells transfected with an HTLV-1 molecular clone (8, 42). As a control, 293T cells transfected with the SV2neo empty vector did not reveal the presence of any particle (Fig. 5d). Budding was also visible in SV2neo$_{PPA-F3}$-transfected 293T cells (Fig. 5e and f).

**SV2neo$_{PPA-F3}$ viral particles are infectious.** Finally, we wanted to determine whether SV2neo$_{PPA-F3}$ particles were or were not infectious. Even though the process is very inefficient, it is possible to infect cells with purified HTLV viruses (17, 18, 28, 42). To determine whether STLV-3$_{PPA-F3}$-transfected cells produce infectious particles, cell culture supernatant was collected from SV2neo$_{PPA-F3}$-transfected cells, purified, and added to 293T-LTR-GFP indicator cells. After several days of culture, a number of syncytia and of GFP-positive cells was observed (Fig. 6a to f). These results demonstrate that the purified STLV-3 particles are infectious. Thermal inactivation is commonly used as a means of efficiently inactivating retroviruses (45). As a control, the STLV-3$_{PPA-F3}$ virus-purified pellet was heated and added to the indicator cells. In that experiment, neither syncytia nor GFP-positive cells were observed (Fig. 6g and h).

## DISCUSSION

The recent discovery of two HTLV-3 strains (7, 63) together with the demonstration of a number of key similarities between the Tax1 and Tax3 proteins (including the presence of a PDZ-binding domain) prompted us to wonder whether this new member of the HTLV group is pathogenic (6). Interestingly, Goubau et al. previously reported the immortalization of human cord blood cells after they were cocultivated with fresh peripheral blood mononuclear cells obtained from STLV-3-infected *Papio hamadryas* monkeys (22). However, until now, a transformed HTLV-3 cell line has not been available for such analysis. We and others have previously shown that HTLV-3 and STLV-3 share the same organization and are highly related in sequence (87 to 99% identity) (6, 11, 55). While the HTLV-3$_{2026ND}$ provirus from the Switzer laboratory has a length that is similar to those of Central African STLV-3 strains (8,917 bp for HTLV-3$_{2026ND}$ versus 8,919 bp for STLV-3$_{CTO-604}$ and 8,916 bp for STLV-3$_{PH969}$), we established that our isolate, HTLV-3$_{Pyl43}$, is shorter, with a 366-bp deletion in the pX-proximal region (6).

Several recent studies of the viral replication or persistence of wild-type or mutant HTLV-1 and HTLV-2 proviruses in vitro or in vivo have benefited from the availability of molecular clones (1, 4, 5, 13, 26, 46, 47, 64–66). Given the high percentage of identity between HTLV-3 and STLV-3 and because the 366-bp pX region that is present in the HTLV-3$_{Pyl43}$ genome deletion (6) seems to be uncommon among PTLV-3 strains, we decided to use an STLV-3 matrix to construct the first PTLV-3 molecular clone. Our construction technique relied on the sequential addition of defined amplified overlapping DNA fragments. Our present results demonstrate that, when transfected into 293T cells, the SV2neo$_{PPA-F3}$ molecular clone is transcribed and can direct the synthesis of viral pro-

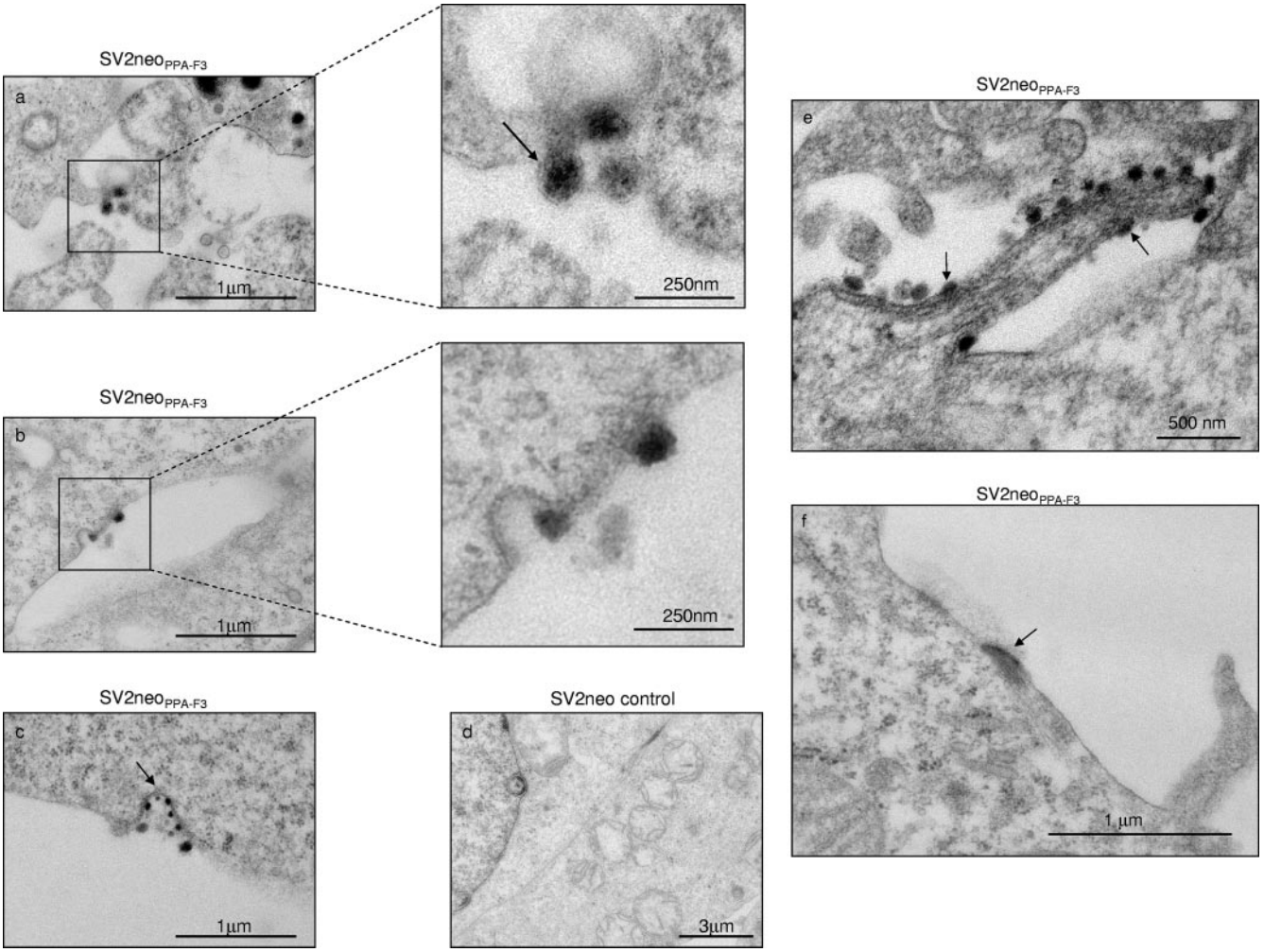


FIG. 5. Electron micrograph showing STLV-3 particles in transiently transfected cells. 293T-LTR-GFP cells were transfected with (a, b, c, e, f) SV2neo$_{PPA-F3}$ or (d) the SV2neo empty vector. Forty-eight hours posttransfection, cell culture medium was removed; the cells were washed with PBS and fixed for ultrastructural analyses as described in Materials and Methods. The images shown are representative of three separate experiments. The arrow in the enlarged area of panel a indicates the presence of an envelope.

teins that are able to assemble to form infectious viral particles as demonstrated by RT-PCR, Western blotting, immunofluorescence imaging, and electron microscopy.

We previously demonstrated that both human and simian Tax3 proteins can transactivate the heterologous HTLV-1 promoter in transient-transfection assays using Tax3 and HTLV-1 reporter plasmids (6, 11). Our current results demonstrate that these results are also true in the context of a genuine infection with an STLV-3 molecular clone that produces Tax3 protein in the infected cells. This suggests that this phenomenon could therefore occur in vivo in individuals dually infected with HTLV-1 and HTLV-3. Whether this would or would not accelerate the occurrence of a disease remains to be determined.

Apart from Tax and Rex, the presence of additional pX gene-encoded proteins in the genomes of STLV-3/HTLV-3 is a matter of debate (36, 37, 57). Apart from *tax* and *rex*, the STLV-3$_{PH969}$ strain was reported to contain at least two putative additional ORFs (RORFI and RORFII) (57). RORFII mRNA could be amplified from STLV-3$_{PH969}$-infected cells, while ORFI could not (57). Subsequently, however, Meertens et al. did not detect the presence of RORFII mRNA in two other STLV-3 samples (STLV-3$_{CTO-604}$ and STLV-3$_{PPA-F3}$) analyzed (36, 37). More recently, in silico analyses from Switzer and colleagues (55) allowed them to report the presence of two putative ORFs (ORFIII and ORFIV) in the HTLV-3 2026ND genome. The SV2neo$_{PPA-F3}$ clone will now give us the unique opportunity to study whether additional (accessory?) pX proteins are encoded by the STLV-3 genome. Similarly, we will now be able to evaluate whether, as is the case for HTLV-1 (20), the complementary strand of the STLV-3 RNA genome encodes a viral protein but also whether the Tax3 PDZ-binding domain that we previously described (11) has any role in vivo.

In conclusion, we have constructed the first PTLV-3 molecular clone. This clone is a unique tool that will now allow us to investigate in vivo the tropism of the STLV-3 virus, the immune response following infection, and the persistence of the virus. One of our next objectives is also to construct an infectious HTLV-3$_{Pyl43}$ molecular clone using the same approach. We have already determined that the 366-bp deletion has no effect on the Tax and Rex ORFs (6); nevertheless, one should

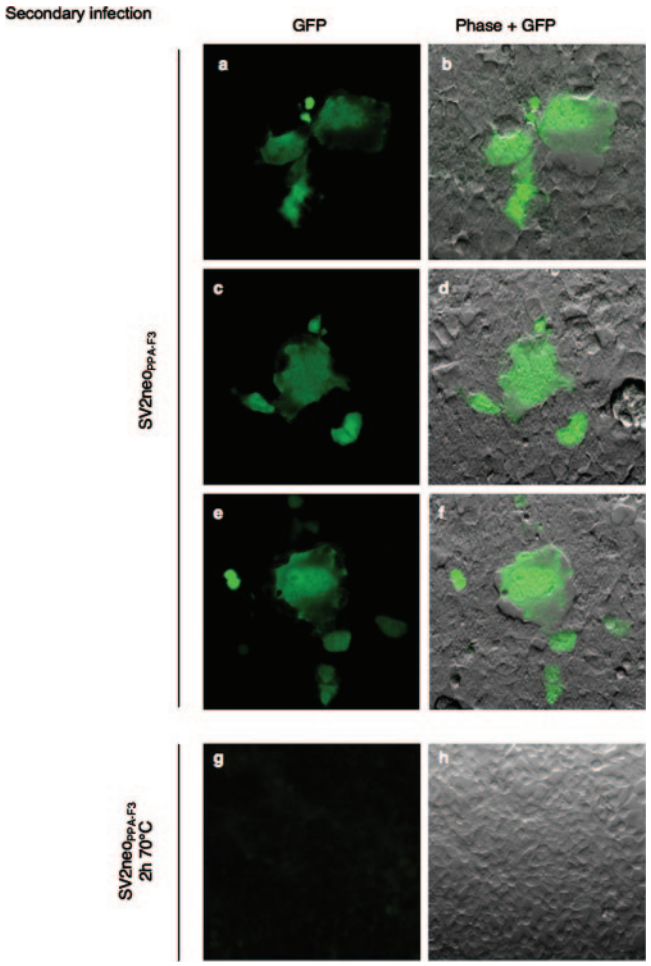


FIG. 6. SV2neo$_{PPA-F3}$ particles are infectious. 293T cells were transfected with SV2neo$_{PPA-F3}$. Forty-eight hours later, growth medium was collected, clarified, and filtered as described in the text. Virus was pelleted by centrifugation and resuspended in DMEM without fetal bovine serum in the presence of 10 μg/ml of DEAE-dextran. Complete medium was then added. One week later, live cells were visualized with a Zeiss Axioplan-Axiocam-ApoTome system (a to f). As a control (g, h), the viral pellet was heated at 70°C for 2 h before being added to the cells. The images shown are representative of two separate experiments.

determine whether this deletion has or does not have an impact on the viral life cycle.

## ACKNOWLEDGMENTS

This work was supported by fellowships from le Ministère de la Recherche and La Fondation pour la Recherche Médicale to S.A.C. and from la Ligue Contre le Cancer to S.C. R.M. is supported by INSERM. Support from the Virus Cancer Prevention Association is also acknowledged.

We thank Pierre Charneau, Fatah Kashanchi, and Tim Stinear for their helpful comments, Patrick Green for the generous gift of the SV2neo and PH6neo plasmids, Pierre-Emmanuel Ceccaldi for the help with the HTLV-1-infected cells micrographs, and Joël Fagot for the STLV-3-infected blood samples.

## REFERENCES

1. **Albrecht, B., N. D. Collins, M. T. Burniston, J. W. Nisbet, L. Ratner, P. L. Green, and M. D. Lairmore.** 2000. Human T-lymphotropic virus type 1 open reading frame I p12$^{I}$ is required for efficient viral infectivity in primary lymphocytes. J. Virol. **74:**9828–9835.
2. **Albrecht, B., and M. D. Lairmore.** 2002. Critical role of human T-lymphotropic virus type 1 accessory proteins in viral replication and pathogenesis. Microbiol. Mol. Biol. Rev. **66:**396–406.
3. **Anderson, M., and P. L. Green.** 2005. Growth and manipulation of a human T-cell leukemia virus type 2 full-length molecular clone. Methods Mol. Biol. **304:**409–421.
4. **Arnold, J., B. Yamamoto, M. Li, A. J. Phipps, I. Younis, M. D. Lairmore, and P. L. Green.** 2006. Enhancement of infectivity and persistence in vivo by HBZ, a natural antisense coded protein of HTLV-1. Blood **107:**3976–3982.
5. **Bartoe, J. T., B. Albrecht, N. D. Collins, M. D. Robek, L. Ratner, P. L. Green, and M. D. Lairmore.** 2000. Functional role of pX open reading frame II of human T-lymphotropic virus type 1 in maintenance of viral loads in vivo. J. Virol. **74:**1094–1100.
6. **Calattini, S., S. A. Chevalier, R. Duprez, P. Afonso, A. Froment, A. Gessain, and R. Mahieux.** 2006. Human T-cell lymphotropic virus type 3: complete nucleotide sequence and characterization of the human Tax3 protein. J. Virol. **80:**9876–9888.
7. **Calattini, S., S. A. Chevalier, R. Duprez, S. Bassot, A. Froment, R. Mahieux, and A. Gessain.** 2005. Discovery of a new human T-cell lymphotropic virus (HTLV-3) in Central Africa. Retrovirology **2:**30.
8. **Ceccaldi, P. E., F. Delebecque, M. C. Prevost, A. Moris, J. P. Abastado, A. Gessain, O. Schwartz, and S. Ozden.** 2006. DC-SIGN facilitates fusion of dendritic cells with human T-cell leukemia virus type 1-infected cells. J. Virol. **80:**4771–4780.
9. **Chen, I. S., J. McLaughlin, J. C. Gasson, S. C. Clark, and D. W. Golde.** 1983. Molecular characterization of genome of a novel human T-cell leukaemia virus. Nature **305:**502–505.
10. **Chevalier, S. A., L. Meertens, S. Calattini, A. Gessain, L. Kiemer, and R. Mahieux.** 2005. Presence of a functional but dispensable nuclear export signal in the HTLV-2 Tax protein. Retrovirology **2:**70.
11. **Chevalier, S. A., L. Meertens, C. Pise-Masison, S. Calattini, H. Park, A. A. Alhaj, M. Zhou, A. Gessain, F. Kashanchi, J. N. Brady, and R. Mahieux.** 2006. The tax protein from the primate T-cell lymphotropic virus type 3 is expressed in vivo and is functionally related to HTLV-1 Tax rather than HTLV-2 Tax. Oncogene **25:**4470–4482.
12. **Ciminale, V., G. N. Pavlakis, D. Derse, C. P. Cunningham, and B. K. Felber.** 1992. Complex splicing in the human T-cell leukemia virus (HTLV) family of retroviruses: novel mRNAs and proteins produced by HTLV type I. J. Virol. **66:**1737–1745.
13. **Collins, N. D., G. C. Newbound, B. Albrecht, J. L. Beard, L. Ratner, and M. D. Lairmore.** 1998. Selective ablation of human T-cell lymphotropic virus type 1 p12I reduces viral infectivity in vivo. Blood **91:**4701–4707.
14. **Delamarre, L., A. R. Rosenberg, C. Pique, D. Pham, and M. C. Dokhelar.** 1997. A novel human T-leukemia virus type 1 cell-to-cell transmission assay permits definition of SU glycoprotein amino acids important for infectivity. J. Virol. **71:**259–266.
15. **Delebecque, F., K. Pramberger, M. C. Prevost, M. Brahic, and F. Tangy.** 2002. A chimeric human T-cell lymphotropic virus type 1 with the envelope glycoprotein of Moloney murine leukemia virus is infectious for murine cells. J. Virol. **76:**7883–7889.
16. **Derse, D., S. A. Hill, P. A. Lloyd, H. Chung, and B. A. Morse.** 2001. Examining human T-lymphotropic virus type 1 infection and replication by cell-free infection with recombinant virus vectors. J. Virol. **75:**8461–8468.
17. **Derse, D., J. Mikovits, M. Polianova, B. K. Felber, and F. Ruscetti.** 1995. Virions released from cells transfected with a molecular clone of human T-cell leukemia virus type I give rise to primary and secondary infections of T cells. J. Virol. **69:**1907–1912.
18. **Derse, D., J. Mikovits, and F. Ruscetti.** 1997. X-I and X-II open reading frames of HTLV-I are not required for virus replication or for immortalization of primary T-cells in vitro. Virology **237:**123–128.
19. **Derse, D., J. Mikovits, D. Waters, S. Brining, and F. Ruscetti.** 1996. Examining the molecular genetics of HTLV-I with an infectious molecular clone of the virus and permissive cell culture systems. J. Acquir. Immune Defic. Syndr. Hum. Retrovirol. **12:**1–5.
20. **Gaudray, G., F. Gachon, J. Basbous, M. Biard-Piechaczyk, C. Devaux, and J. M. Mesnard.** 2002. The complementary strand of the human T-cell leukemia virus type 1 RNA genome encodes a bZIP transcription factor that down-regulates viral transcription. J. Virol. **76:**12813–12822.
21. **Ghez, D., Y. Lepelletier, S. Lambert, J. M. Fourneau, V. Blot, S. Janvier, B. Arnulf, P. M. van Endert, N. Heveker, C. Pique, and O. Hermine.** 2006. Neuropilin-1 is involved in human T-cell lymphotropic virus type 1 entry. J. Virol. **80:**6844–6854.
22. **Goubau, P., M. Van Brussel, A. M. Vandamme, H. F. Liu, and J. Desmyter.** 1994. A primate T-lymphotropic virus, PTLV-L, different from human T-lymphotropic viruses types I and II, in a wild-caught baboon (Papio hamadryas). Proc. Natl. Acad. Sci. USA **91:**2848–2852.
23. **Green, P. L., T. M. Ross, I. S. Chen, and S. Pettiford.** 1995. Human T-cell leukemia virus type II nucleotide sequences between *env* and the last exon of *tax*/*rex* are not required for viral replication or cellular transformation. J. Virol. **69:**387–394.
24. **Green, P. L., Y. M. Xie, and I. S. Chen.** 1990. The internal methionine codons

of human T-cell leukemia virus type II *rex* gene are not required for p24$^{rex}$ production or virus replication and transformation. J. Virol. **64:**4914–4921.
25. **Guo, H. G., F. Wong-Stall, and R. C. Gallo.** 1984. Novel viral sequences related to human T-cell leukemia virus in T cells of a seropositive baboon. Science **223:**1195–1197.
26. **Hiraragi, H., S. J. Kim, A. J. Phipps, M. Silic-Benussi, V. Ciminale, L. Ratner, P. L. Green, and M. D. Lairmore.** 2006. Human T-lymphotropic virus type 1 mitochondrion-localizing protein p13$^{II}$ is required for viral infectivity in vivo. J. Virol. **80:**3469–3476.
27. **Jassal, S. R., M. D. Lairmore, A. J. Leigh-Brown, and D. W. Brighty.** 2001. Soluble recombinant HTLV-1 surface glycoprotein competitively inhibits syncytia formation and viral infection of cells. Virus Res. **78:**17–34.
28. **Jinno, A., Y. Haraguchi, H. Shiraki, and H. Hoshino.** 1999. Inhibition of cell-free human T-cell leukemia virus type 1 infection at a postbinding step by the synthetic peptide derived from an ectodomain of the gp21 transmembrane glycoprotein. J. Virol. **73:**9683–9689.
29. **Jones, K. S., K. Fugo, C. Petrow-Sadowski, Y. Huang, D. C. Bertolette, I. Lisinski, S. W. Cushman, S. Jacobson, and F. W. Ruscetti.** 2006. Human T-cell leukemia virus type 1 (HTLV-1) and HTLV-2 use different receptor complexes to enter T cells. J. Virol. **80:**8291–8302.
30. **Jones, K. S., C. Petrow-Sadowski, D. C. Bertolette, Y. Huang, and F. W. Ruscetti.** 2005. Heparan sulfate proteoglycans mediate attachment and entry of human T-cell leukemia virus type 1 virions into CD4$^+$ T cells. J. Virol. **79:**12692–12702.
31. **Kim, F. J., N. Manel, Y. Boublik, J. L. Battini, and M. Sitbon.** 2003. Human T-cell leukemia virus type 1 envelope-mediated syncytium formation can be activated in resistant mammalian cell lines by a carboxy-terminal truncation of the envelope cytoplasmic domain. J. Virol. **77:**963–969.
32. **Kimata, J. T., F. H. Wong, J. J. Wang, and L. Ratner.** 1994. Construction and characterization of infectious human T-cell leukemia virus type 1 molecular clones. Virology **204:**656–664.
33. **Li, Q. X., D. Camerini, Y. Xie, M. Greenwald, D. R. Kuritzkes, and I. S. Chen.** 1996. Syncytium formation by recombinant HTLV-II envelope glycoprotein. Virology **218:**279–284.
34. **Manel, N., F. J. Kim, S. Kinet, N. Taylor, M. Sitbon, and J. L. Battini.** 2003. The ubiquitous glucose transporter GLUT-1 is a receptor for HTLV. Cell **115:**449–459.
35. **Meertens, L., S. Chevalier, R. Weil, A. Gessain, and R. Mahieux.** 2004. A 10-amino acid domain within HTLV-1 and HTLV-2 Tax protein sequences is responsible for their divergent subcellular localization. J. Biol. Chem. **279:**43307–43320.
36. **Meertens, L., and A. Gessain.** 2003. Divergent simian T-cell lymphotropic virus type 3 (STLV-3) in wild-caught *Papio hamadryas papio* from Senegal: widespread distribution of STLV-3 in Africa. J. Virol. **77:**782–789.
37. **Meertens, L., R. Mahieux, P. Mauclere, J. Lewis, and A. Gessain.** 2002. Complete sequence of a novel highly divergent simian T-cell lymphotropic virus from wild-caught red-capped mangabeys (*Cercocebus torquatus*) from Cameroon: a new primate T-lymphotropic virus type 3 subtype. J. Virol. **76:**259–268.
38. **Miyauchi, M., and K. Maruyama.** 1990. Morphological and antigenic variations of human T cell leukemia virus type I particles in human lymphocytes. J. Electron Microsc. (Tokyo) **39:**145–154.
39. **Nicot, C., T. Astier-Gin, E. Edouard, E. Legrand, D. Moynet, A. Vital, D. Londos-Gagliardi, J. P. Moreau, and B. Guillemain.** 1993. Establishment of HTLV-I-infected cell lines from French, Guianese and West Indian patients and isolation of a proviral clone producing viral particles. Virus Res. **30:**317–334.
40. **Nicot, C., M. Dundr, J. M. Johnson, J. R. Fullen, N. Alonzo, R. Fukumoto, G. L. Princler, D. Derse, T. Misteli, and G. Franchini.** 2004. HTLV-1-encoded p30II is a post-transcriptional negative regulator of viral replication. Nat. Med. **10:**197–201.
41. **Nicot, C., R. L. Harrod, V. Ciminale, and G. Franchini.** 2005. Human T-cell leukemia/lymphoma virus type 1 nonstructural genes and their functions. Oncogene **24:**6026–6034.
42. **Ohsugi, T., T. Kumasaka, and T. Urano.** 2004. Construction of a full-length human T cell leukemia virus type I genome from MT-2 cells containing multiple defective proviruses using overlapping polymerase chain reaction. Anal. Biochem. **329:**281–288.
43. **Poiesz, B. J., F. W. Ruscetti, A. F. Gazdar, P. A. Bunn, J. D. Minna, and R. C. Gallo.** 1980. Detection and isolation of type C retrovirus particles from fresh and cultured lymphocytes of a patient with cutaneous T-cell lymphoma. Proc. Natl. Acad. Sci. USA **77:**7415–7419.
44. **Poiesz, B. J., F. W. Ruscetti, M. S. Reitz, V. S. Kalyanaraman, and R. C. Gallo.** 1981. Isolation of a new type C retrovirus (HTLV) in primary uncultured cells of a patient with Sezary T-cell leukaemia. Nature **294:**268–271.
45. **Quinnan, G. V., Jr., M. A. Wells, A. E. Wittek, M. A. Phelan, R. E. Mayner, S. Feinstone, R. H. Purcell, and J. S. Epstein.** 1986. Inactivation of human T-cell lymphotropic virus, type III by heat, chemicals, and irradiation. Transfusion **26:**481–483.
46. **Robek, M. D., and L. Ratner.** 2000. Immortalization of T lymphocytes by human T-cell leukemia virus type 1 is independent of the Tax-CBP/p300 interaction. J. Virol. **74:**11988–11992.
47. **Robek, M. D., F. H. Wong, and L. Ratner.** 1998. Human T-cell leukemia virus type 1 pX-I and pX-II open reading frames are dispensable for the immortalization of primary lymphocytes. J. Virol. **72:**4458–4462.
48. **Seiki, M., S. Hattori, Y. Hirayama, and M. Yoshida.** 1983. Human adult T-cell leukemia virus: complete nucleotide sequence of the provirus genome integrated in leukemia cell DNA. Proc. Natl. Acad. Sci. USA **80:**3618–3622.
49. **Shimotohno, K., D. W. Golde, M. Miwa, T. Sugimura, and I. S. Chen.** 1984. Nucleotide sequence analysis of the long terminal repeat of human T-cell leukemia virus type II. Proc. Natl. Acad. Sci. USA **81:**1079–1083.
50. **Shimotohno, K., Y. Takahashi, N. Shimizu, T. Gojobori, D. W. Golde, I. S. Chen, M. Miwa, and T. Sugimura.** 1985. Complete nucleotide sequence of an infectious clone of human T-cell leukemia virus type II: an open reading frame for the protease gene. Proc. Natl. Acad. Sci. USA **82:**3101–3105.
51. **Shimotohno, K., W. Wachsman, Y. Takahashi, D. W. Golde, M. Miwa, T. Sugimura, and I. S. Chen.** 1984. Nucleotide sequence of the 3′ region of an infectious human T-cell leukemia virus type II genome. Proc. Natl. Acad. Sci. USA **81:**6657–6661.
52. **Silverman, L. R., A. J. Phipps, A. Montgomery, L. Ratner, and M. D. Lairmore.** 2004. Human T-cell lymphotropic virus type 1 open reading frame II-encoded p30II is required for in vivo replication: evidence of in vivo reversion. J. Virol. **78:**3837–3845.
53. **Slamon, D. J., M. F. Press, L. M. Souza, D. C. Murdock, M. J. Cline, D. W. Golde, J. C. Gasson, and I. S. Chen.** 1985. Studies of the putative transforming protein of the type I human T-cell leukemia virus. Science **228:**1427–1430.
54. **Slamon, D. J., K. Shimotohno, M. J. Cline, D. W. Golde, and I. S. Chen.** 1984. Identification of the putative transforming protein of the human T-cell leukemia viruses HTLV-I and HTLV-II. Science **226:**61–65.
55. **Switzer, W. M., S. H. Qari, N. D. Wolfe, D. S. Burke, T. M. Folks, and W. Heneine.** 2006. Ancient origin and molecular features of the novel human T-lymphotropic virus type 3 revealed by complete genome analysis. J. Virol. **80:**7427–7438.
56. **Takemura, T., M. Yamashita, M. K. Shimada, S. Ohkura, T. Shotake, M. Ikeda, T. Miura, and M. Hayami.** 2002. High prevalence of simian T-lymphotropic virus type L in wild Ethiopian baboons. J. Virol. **76:**1642–1648.
57. **Van Brussel, M., P. Goubau, R. Rousseau, J. Desmyter, and A. M. Vandamme.** 1996. The genomic structure of a new simian T-lymphotropic virus, STLV-PH969, differs from that of human T-lymphotropic virus types I and II. J. Gen. Virol. **77:**347–358.
58. **Van Dooren, S., L. Meertens, P. Lemey, A. Gessain, and A. M. Vandamme.** 2005. Full-genome analysis of a highly divergent simian T-cell lymphotropic virus type 1 strain in Macaca arctoides. J. Gen. Virol. **86:**1953–1959.
59. **Van Dooren, S., V. Shanmugam, V. Bhullar, B. Parekh, A. M. Vandamme, W. Heneine, and W. M. Switzer.** 2004. Identification in gelada baboons (Theropithecus gelada) of a distinct simian T-cell lymphotropic virus type 3 with a broad range of Western blot reactivity. J. Gen. Virol. **85:**507–519.
60. **Vincent, M. J., F. J. Novembre, V. F. Yamshchikov, H. M. McClure, and R. W. Compans.** 1996. Characterization of a novel baboon virus closely resembling human T-cell leukemia virus. Virology **226:**57–65.
61. **Wang, B., M. G. Agadjanyan, V. Srikantan, K. E. Ugen, W. Hall, M. H. Kaplan, K. Dang, W. V. Williams, and D. B. Weiner.** 1993. Molecular cloning, expression, and biological characterization of an HTLV-II envelope glycoprotein: HIV-1 expression is permissive for HTLV-II-induced cell fusion. AIDS Res. Hum. Retrovir. **9:**849–860.
62. **Wirtz, R., and M. Lochelt.** 2005. Construction and analysis of genomic, full-length infectious foamy virus DNA clones. Methods Mol. Biol. **304:**423–434.
63. **Wolfe, N. D., W. Heneine, J. K. Carr, A. D. Garcia, V. Shanmugam, U. Tamoufe, J. N. Torimiro, A. T. Prosser, M. Lebreton, E. Mpoudi-Ngole, F. E. McCutchan, D. L. Birx, T. M. Folks, D. S. Burke, and W. M. Switzer.** 2005. Emergence of unique primate T-lymphotropic viruses among central African bushmeat hunters. Proc. Natl. Acad. Sci. USA **102:**7994–7999.
64. **Xie, L., B. Yamamoto, A. Haoudi, O. J. Semmes, and P. L. Green.** 2006. PDZ binding motif of HTLV-1 Tax promotes virus-mediated T-cell proliferation in vitro and persistence in vivo. Blood **107:**1980–1988.
65. **Ye, J., L. Xie, and P. L. Green.** 2003. Tax and overlapping Rex sequences do not confer the distinct transformation tropisms of human T-cell leukemia virus types 1 and 2. J. Virol. **77:**7728–7735.
66. **Younis, I., B. Yamamoto, A. Phipps, and P. L. Green.** 2005. Human T-cell leukemia virus type 1 expressing nonoverlapping Tax and Rex genes replicates and immortalizes primary human T lymphocytes but fails to replicate and persist in vivo. J. Virol. **79:**14473–14481.
67. **Zemba, M., A. Alke, J. Bodem, I. G. Winkler, R. L. Flower, K. Pfrepper, H. Delius, R. M. Flugel, and M. Lochelt.** 2000. Construction of infectious feline foamy virus genomes: cat antisera do not cross-neutralize feline foamy virus chimera with serotype-specific Env sequences. Virology **266:**150–156.
68. **Zhao, T. M., M. A. Robinson, F. S. Bowers, and T. J. Kindt.** 1995. Characterization of an infectious molecular clone of human T-cell leukemia virus type I. J. Virol. **69:**2024–2030.